J Solid State Electrochem (2008) 12:1573–1577
DOI 10.1007/s10008-008-0514-6

ORIGINAL PAPER

Electrochemical reduction of NO and O_2 on $La_{2-x}Sr_xCuO_4$-based electrodes

Vibe L. E. Simonsen · Linda Nørskov · Kent Kammer Hansen

Received: 24 September 2007 / Revised: 4 January 2008 / Accepted: 9 January 2008 / Published online: 12 February 2008

Abstract A series of $La_{2-x}Sr_xCuO_4$ ($x = 0.0, 0.05, 0.15, 0.25$ and 0.35) compounds was investigated for the use of direct electrochemical reduction of NO in an all-solid-state electrochemical cell. The materials were investigated using cyclic voltammetry in 1% NO in Ar and 10% O_2 in Ar. The most selective electrode material was La_2CuO_4, which had an activity of NO reduction that was 6.8 times higher than that of O_2 at 400 °C. With increasing temperature, activity increased while selectivity decreased. Additionally, conductivity measurements were carried out, and the materials show metallic conductivity behavior which follows an adiabatic small polaron hopping mechanism.

Keywords Electrochemical reduction · NO · Cone-shaped electrodes · K_2NiF_4 structure · $La_{2-x}Sr_xCuO_4$

Introduction

Lean-burned fired diesel engines can increase fuel efficiency approximately 30% compared to petrol-fired engines, which makes them attractive for road traffic vehicles because of the increase in oil prices. Unfortunately, diesel-fired engines emit large amounts of NO_x and road traffic accounts for 32% of all NO_x emitted in the EU [1]. Increasing environmental concern has lead to a demand for decreasing the emission of NO_x, SO_x, and carbon particulate, and the regulation for emissions is becoming more and more strict (www.dieselnet.com/standards/eu/hd.html, www.dieselnet.com/standards/eu/ld.html). Several methods exist for removing NO_x from the exhaust gas, and the most well known are selective catalytic reduction (SCR) as urea-SCR [2] or HC-SCR [3] and BaO storage catalysts [4]. At the moment, none of the listed techniques can reach the future emission standards. An alternative method for removing NO_x is by electrochemistry, which was initially discovered by Pancharatnam et al. in 1975 on Pt electrodes [5]. At the cathode, NO_x is reduced electrochemically to N_2 and O^{2-} ions. The O^{2-} ions are transported through an oxide ion conductor to the anode, where O^{2-} is oxidized to O_2. The major obstacle with this technique is the competing reduction reaction of O_2 at the cathode, which leads to a decrease in current efficiency.

This study investigates $La_{2-x}Sr_xCuO_4$ ($x = 0$, 0.05, 0.15, 0.25, and 0.35) compounds as possible cathode materials for selective electrochemical reduction of NO. $La_{2-x}Sr_xCuO_4$ compounds have the K_2NiF_4 structure and have been studied for direct decomposition of NO by Yasuda et al. [6]. Zhen et al. [7] showed that it is the oxygen vacancies that are active for the direct decomposition of NO and not the amount of Cu^{3+} ions.

V. L. E. Simonsen (✉) · L. Nørskov · K. K. Hansen
Fuel Cells and Solid State Chemistry Department,
National Laboratory for Sustainable Energy,
Technical University of Denmark, Frederiksborgvej 399 - building 227, 4000 Roskilde, Denmark
e-mail: vibe.simonsen@risoe.dk

Experimental procedure

The $La_{2-x}Sr_xCuO_4$ series was synthesized in-house by the glycine nitrate route described by Chick et al. [8]. The nitrate solutions were prepared using $La(NO_3)_3$,

$Sr(NO_3)_2$, and $Cu(NO_3)_2$ (Alfa Aesar, 99.9, 99.0, and 99.0%, respectively). After synthesis, the produced powders were ball-milled for 24 h before being calcined at 900 °C for 6 h. The structure and phase purity of the calcined powder was checked using an X-ray diffractometer (STOE Theta—Theta diffractometer). The X-ray diffractograms were collected at $10° \leq 2\theta \leq 120°$, step size 0.05° with CuK_α radiation. The International Centre for Diffraction Data database was used to determine the phases present in the $La_{2-x}Sr_xCuO_4$ sample. The sample for $x = 0.35$ was not completely single-phase and was calcined once more at 1,000 °C for 6 h.

After X-ray showed a singled phased structure of K_2NiF_4, the powder was uniaxially pressed into pellets at 1 ton in an appropriate dye. The pellets were then subjected to isostatic pressure of 50 tons to become more dense and obtain mechanical strength. To strengthen the pellets further, they were sintered for 12 h at 1,000 °C for the pellets where $x = 0$, 0.05 and, 0.15. The $x = 0.25$ and 0.35 pellets were sintered at 800 °C for 12 h, as higher temperatures led to large porosities and cracks. After sintering, the pellets were mechanically tooled into cone-shaped electrodes or bars for conductivity measurements with a diamond tool. Before any measurements were conducted on electrodes or bars, they were subjected to an ultrasonic bath for 20 min in ethanol to remove any remains in the form of oil and metallic splinters from the mechanical tooling.

For classifying the electrochemical NO reduction properties of the $La_{2-x}Sr_xCuO_4$ compounds, a pseudo three-electrode setup was used at 400, 500, and 600 °C, as described elsewhere [9]. The working electrode was the cone-shaped electrode described in the previous section. The cone electrode was pressed against the electrolyte with 60-g weights, and the electrolyte was the bottom of a 10.5% yttria stabilized zirconia (YSZ) one-end-closed tube from Visuvius. The combined counter and reference electrode was Ag-paste (Ferro, 6122 0002) smeared directly on the inside of the closed end of the YSZ tube. The counter/reference electrode was subjected to air, which works as the reference gas, and the electrode was connected to the surroundings with a Pt/PtRh thermocouple, which allows the temperature of the setup to be monitored. In all experiments, the working electrode was subjected to 1% NO in Ar (certified to ±2% from Air Liquide) or 10% O_2 in Ar from Air Liquide. The gas flow was kept at 25 $\frac{\text{ml}}{\text{min}}$ by Brooks mass flow controllers. The temperature of the oven was controlled by a EuroTherm temperature controller. The temperature was measured directly on the anode before each experiment to ensure that the cone-shaped electrode–electrolyte–counter electrode was at the correct temperature.

Cyclic voltammograms were run in the potential range −0.5 to 0.5 V vs Ag/air with a sweeprate of 1 $\frac{\text{mV}}{\text{s}}$ as the current response for a given potential was a direct measure of the conversion of NO and O_2, respectively. The cycles were initiated at open circuit voltage and run in cathodic direction before running in the anodic direction. To compare the electrode materials directly, the current responses were corrected to current densities by use of the contact area between cone-shaped electrode and the electrolyte. The contact area was determined by impedance spectroscopy (Solartron 1255b + 1287, frequency analyzer, range 0.05 Hz–700 kHz, 20 points per decade, and an amplitude of 25 mA) in combination with Newman's formula [10], see Eq. 1.

$$r = \frac{1}{4\sigma R_s} \tag{1}$$

Newman's formula assumes that the contact area is circular and r is the radius of the contact area i cm, σ is the specific conductivity of the electrolyte material given in siemens per centimeter, and R_s is the electrolyte resistance in ohms. The specific conductivity of the electrolyte material can be determined from Eq. 2 reported by Appel et al. [11] for a similar material.

$$\sigma = \frac{1.51 \cdot 10^6}{T} \cdot e^{\frac{-0.94eV}{kT}} \tag{2}$$

where σ is the specific conductivity in siemens per centimeter and T and k are the temperature in degrees Kelvin and Boltzman's constant, respectively. The area of the tip of the cone-shaped electrode varies from 10^{-3} and 10^{-6} cm^2 from electrode to electrode.

Four-point DC resistivity measurements were conducted on sintered bars of $4 \times 4 \times 18$ mm. Two wires were attached to the bar with Pt paste and sintered for 2 h at 1,000 °C to fix the wires. Additionally, two Pt probes were pressed against the bar with spring loads and a well known length between them. The two wires attached with Pt paste were used to send a known DC current through the sample, and the voltage drop was measured across the two remaining wires. The resistivity was measured every 15 min from 50 to 1,000 °C and back to 50 °C. There was a 2-h dwell every 50 °C, and the rate of heating/cooling was 2 $\frac{^\circ\text{C}}{\text{min}}$.

Results and discussion

The ability to reduce NO before O_2 is an important property of the electrode material as it should

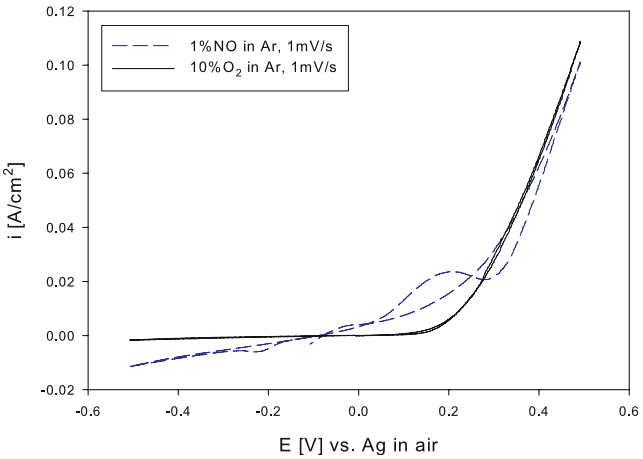

Fig. 1 CV for the second cycles at 400 °C for a La_2CuO_4 electrode. The measurements are performed in 10% O_2 in Ar and 1% NO in Ar at 1 $\frac{mV}{s}$

show selective catalytic behavior for the two competing reduction reactions. In addition the electrode material must be an acceptable electron conductor to work as an electrode.

Electrochemical reduction properties

Cyclic voltammograms (CV) were recorded for all the materials to determine the degree of conversion as a function of applied potential. The CV for the second cycle for La_2CuO_4 is shown in Fig. 1. Figure 1 shows a reduction peak at −0.225 V vs Ag in air and two oxidation peaks at −0.033 V vs Ag in air and 0.19 V vs Ag in air, respectively. The potentials for reducing CuO to Cu_2O and Cu were calculated in FactSage [12] and found to be −0.34 and −0.47 V vs air, respectively. Thus, it is not likely that it is Cu^{2+} in the electrode material itself which is reduced. Instead, the reduction of Cu^{3+} to Cu^{2+} would be a more probable suggestion, although we do not expect any Cu^{3+} to be present in the sample. What does verify the Cu^{3+}-reduction statement is that no reduction peaks were present in the very first cycle run, while oxidation peaks were seen. This indicates the formation of Cu^{3+} during the first cycle, which can subsequently be reduced in the second cycle. When running more sweeps, the data could be reproduced, and it seems that no permanent structural changes occurred in the electrode material. As the content of Sr was increased, the peaks became smaller, and at $x > 0.15$, the peaks were not observed possible due to the increased content of Cu^{3+} or increased amount of oxygen vacancies. On the other hand, increasing the amount of Sr in the electrode material led to lower activities of the electrode for both reduction and oxidation. Running the experiment in 10% O_2 showed no peaks even if additional cycles were run, which indicates the Cu^{2+}/Cu^{3+} redox theory is not correct. On the basis of the results shown in the figure, another possible explanation may be the formation of $Cu(NO_3)_2$. The formation of copper nitrate is only possible after oxygen is pumped through the electrolyte at anodic currents and will thus not be reduced until after the first cycle is run.

Table 1 summarizes the results obtained in this study where the ratio between the current densities for NO and O_2 reduction found at −0.5 V vs air indicates the possible selectivity present in the electrode. For increasing Sr content, the activity of the electrode and ratio of activities decreased leading to the conclusion that La_2CuO_4 was the best electrode of the tested materials. When the temperature was increased 100 °C, the measured current densities of the electrode increased approximately by a factor of 10. On the other hand, the ratio between the current densities decreased with increasing temperature, and above 500 °C, the electrodes were approximately as good at reducing O_2 as NO, and thus, selectivity was lost, which has also previously been reported [13]. Kammer et al. [13] suggested that redox capacity in perovskites improved the reduction performance for NO, but this does not seem to be the case for K_2NiF_4 structures containing Cu, as increased content of Sr decreases the ability to reduce NO. Increasing the Cu^{3+}/Cu^{2+} ratio or introducing oxygen vacancies is not beneficial for the reduction of NO. The results indicate

Table 1 Current densities for the $La_{2-x}Sr_xCuO_4$ series in 10% O_2 and 1% NO at 400 °C at an applied potential of −500 mV

Compound	i [A/cm^2] - 1% NO	i [A/cm^2] - 10% O_2	Ratio
La_2CuO_4	$-1.129 \cdot 10^{-2}$	$-1.664 \cdot 10^{-3}$	6.78
$La_{1.95}Sr_{0.05}CuO_4$	$-1.491 \cdot 10^{-3}$	$-2.754 \cdot 10^{-3}$	0.541
$La_{1.85}Sr_{0.15}CuO_4$	$-1.658 \cdot 10^{-3}$	$-4.900 \cdot 10^{-3}$	0.338
$La_{1.75}Sr_{0.25}CuO_4$	$-1.453 \cdot 10^{-3}$	$-5.017 \cdot 10^{-4}$	2.90
$La_{1.65}Sr_{0.35}CuO_4$	$-7.423 \cdot 10^{-4}$	$-2.144 \cdot 10^{-4}$	3.46

The ratio given is the ratio of i_{NO}/i_{O_2} and is an indication of the possible selectivity of the cathode material towards the reduction of NO compared to O_2

that the divalent Cu-ion in the B position must play an important role in the reduction mechanism of NO.

The reduction rate of O_2 at −500 mV reaches a maximum around $x = 0.15$ and decreases to values lower than that of $x = 0.0$. This is probably due to ordering of oxygen vacancies for higher Sr contents, which make the vacancies less mobile, or a decrease in the content of Cu^{2+}. This is not possible to verify from the experiments carried out in this study, and no theory is found supporting this theory for cuprates having the K_2NiF_4 structure. Ordering of oxygen vacancies is, however, a well known phenomena for perovskite-related structures, such as, e.g., $YBa_2Cu_3O_{7+\delta}$ [14].

In the anodic region, O^{2-} is transported from the counter electrode to the working electrode. In an O_2 atmosphere, the current densities will show the ability to release O_2 from the working electrode material. However, in a NO-containing atmosphere, the product can be either the release of O_2, the formation of NO_2, or a mixture. As the gas conversion is very low on cone-shaped electrodes, it is not possible to verify which product is the actual one. What can be seen from the experiments is that O_2 was released at lower potentials in the O_2-containing atmosphere than in the NO-containing atmosphere. This indicates that either NO_2 is more difficult to form than O_2 or NO inhibits the release of O_2. The applied overvoltage needed to obtain an anodic current decreased with increasing temperature. According to thermodynamics, the formation of NO_2 is inhibited at higher temperatures, which leads to the conclusion that it is O_2 that is released in the anodic region. The release of O_2 at lower potentials in the O_2 atmosphere than in the NO atmosphere indicates that NO inhibits the release of O_2.

Analysis of electrical conductivity

The total conductivity of the materials was investigated, as the material is to be used as an electrode material. An Arrhenius plot of the measured conductivities is shown in Fig. 2. The measurements have been corrected for porosity using the Bruggerman asymmetric model [15], as the samples had densities of the theoretical densities of 87.88, 96.03, 94.53, 75.67, and 72.67% for $x = 0$, 0.05, 0.15, 0.25, and 0.35, respectively. As the type of conductivity of the series cannot be determined directly from Fig. 2, the conductivity vs reciprocal temperature was plotted. The plot showed that the series of cuprates exhibited metallic conductivity in the whole temperature range and the conductivity increased with increasing Sr-content for $x \leq 0.25$ and then decreased for $x = 0.35$. These results are in agreement with the results reported by Kanai et al. [16], who tested a

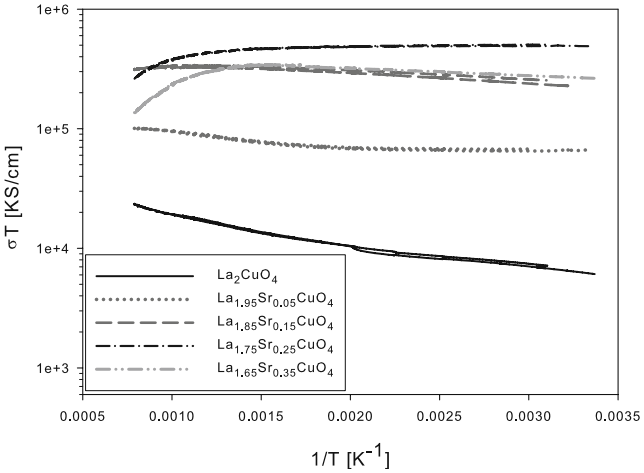

Fig. 2 Conductivities for the $La_{2-x}Sr_xCuO_4$ series obtained by four-point resistivity measurements. The conductivities are corrected for porosities using the Bruggerman asymmetric model

$La_{2-x}Sr_xCuO_4$ series with $x = 0$–0.3. The increase in conductivity as a function of Sr content is assumed to be due to an increase in the concentration and mobility of electronic holes associated with Cu^{3+} compared to Cu^{2+}. The decrease in conductivity for the $x = 0.35$ sample may be described by the increase in oxygen vacancies and the corresponding decoupling of the oxygen p-orbital, metal d-orbital, oxygen p-orbital super-exchange. On the other hand, the sample was highly porous, and therefore, this could also be the reason for the diversity from the general trend of the series, as the measurements may be inaccurate. The deviation from linearity at high temperatures for the compounds with $x = 0.25$ and $x = 0.35$ is due to the increase in oxygen vacancies and, thus, the decoupling of the oxygen p-orbital, metal d-orbital, oxygen p-orbital super-exchange. Furthermore, Cu^{3+} is reduced to Cu^{2+} at high temperatures and is, thus, more pronounced for the compounds with high Sr-content.

Above approximately 400 °C, the materials stopped exhibiting Arrhenius behavior and the slope became numerically larger. For $x = 0.0$ and $x = 0.05$, the resistivity behavior was different from the cuprates with higher Sr-content. This was most likely because of an orthorombic phase in the low Sr-content compounds, whereas the high-Sr-content compounds had tetragonal phase. Furthermore, decoupling of the super-exchange occurred when the amount of Cu^{3+} charge carrier was decreased. Kanai et al. [16] reported a shift for $x = 0$ and $x = 0.05$ from orthorombic to tetragonal phase at 506–536 °C, whereas we observed the change at 230 °C. The phase change was observed as plateaus in the range 150–250 °C for the two compounds, and the plateaus disappeared when the Sr-content was increased and

Table 2 Activation energies for the conductivity of the $La_{2-x}Sr_xCuO_4$ series in air in the temperature range 25–600 °C

Compound	E_a [eV]
$x = 0$	0.0938
$x = 0.05$	0.0592
$x = 0.15$	0.0725
$x = 0.25$	0.0667
$x = 0.35$	0.0581

the phase was tetragonal throughout the whole temperature range. The difference in temperature of the phase changes is probably due to the different methods of synthesis and, thus, oxygen stoichiometry in the results reported by Kanai et al. [16]. The electrical conductivities of the tested cuprates were in the range of those of perovskites used in fuel cells. That makes them acceptable for the purpose of electrodes in an electrochemical cell [17].

The conductivity behavior beneath a certain characteristic temperature (the linear range in Fig. 2) indicates that the conductivity follows Eq. 3. Equation 3 describes the conductivity due to the small polaron hopping mechanism [18].

$$\sigma = \frac{A}{kT^{\nu}} exp\left\{\frac{-E_a}{kT}\right\} \tag{3}$$

where T is the temperature, A is a materials constant, k is Boltzmann's constant, and E_a is the activation energy for anion vacancy migration. The exponent $\nu = 1$ for adiabatic small polaron hopping and $\nu = \frac{3}{2}$ for the process of nonadiabatic small polaron hopping. For the results shown in Fig. 2, the adiabatic case of $\nu = \frac{3}{2}$ fits the data best, and the activation energies are summarized in Table 2.

Conclusion

La_2CuO_4 electrode material was best for the electrochemical reduction of NO, as it showed the highest activity towards NO compared to O_2. The ability to reduce NO compared to O_2 decreased with increasing temperature, while the overall activity increased with increasing temperature. A small increase in Sr content decreased selectivity, while a further increase in Sr content increased the selectivity. Unfortunately, La_2CuO_4 had the lowest conductivity of the tested series of materials, which all showed metallic conductivity behavior and followed an adiabatic polaron hopping mechanism.

Acknowledgements We would like to thank the staff at the Fuel Cells and Solid State Chemistry Department, Risø National Laboratory, especially Dr. M. Mogensen and Dr. Martin Søgaard for many fruitful discussions and help in the lab.

References

1. Klingstedt F, Arve K, Eränen K, Murzin DY (2006) Acc Chem Res 39:273
2. Ciardellia C, Novaa I, Tronconia E, Chatterjeeb D, Bandl-Konradb B, Weibelb M, Krutzsch B (2007) Appl Catal B Environ 70:80
3. Breen JP, Burch RA (2006) Top Catal 39:53
4. Dawody J, Skoglundh M, Olsson L, Fridell E (2007) Appl Catal B Environ 70:179
5. Pancharatnam S, Huggins RA, Mason DM (1975) J Electrochem Soc 122:869
6. Yasuda H, Nitadori T, MiZuno N (1991) Nippon Kagaku Kaishi 5:604
7. Zhen Z, Xiangguang Y, Yue W (1996) J Rare Earths 14:241
8. Chick LA, Pederson LR, Maupin GD, Bates JL, Thomas LE, Exarhos GJ (1990) Mater Lett 10:6
9. Hansen KK, Christensen H, Skou EM, Skaarup SV (2000) J Appl Electrochem 30:193
10. Newman J (1966) J Electrochem Soc 113:501
11. Appel CC, Bonanos N, Horsewell A, Linderoth S (2001) J Mater Sci 36:4493
12. ThermFact (2004) FactSage (version 5.3.1). ThermFact, Montreal
13. Kammer Hansen K, Skou EM, Christensen H (2000) J Electrochem Soc 147:2007
14. Alario-Franco MA, Chaillout C, Capponi JJ, Chenavas J (1987) Mater Res Bull 22:1685
15. Bruggeman DAG (1935) Ann Phys 24:635
16. Kanai H, Hashimoto T, Tagawa H, Mizusaki J (2000) Electrochemistry 68:507
17. Poulsen FW (2000) Solid State Ion 129:145
18. Wimmer JM, Bransky I (1971) In: Tallan NM (ed) Electrical conductivity in ceramics and glass, chapter 4. Pergamon, New York